Agronomy Research **18**(3), 2166–2184, 2020
https://doi.org/10.15159/AR.20.164

Thermal performance of a solar hybrid dryer for Conilon coffee (*Coffea canephora*)

J.L. Paes[1,*], B.C. Vargas[1], J.P.B. Cunha[1], D.S.C. Silva[1], G.A.S. Ferraz[2], M.R.S. Braz[1], P.F.P. Ferraz[2], L. Conti[3] and G. Rossi[3]

[1]Rural Federal University of Rio de Janeiro, Engineering Department, Campus Seropédica, ZIP Code BR23890000, Seropédica, Rio de Janeiro, Brazil
[2]Federal University of Lavras, Agricultural Engineering Department, ZIP Code BR37200000, Lavras, Minas Gerais, Brazil
[3]University of Florence, Department of Agricultural, Food, Environment and Forestry (DAGRI), Via San Bonaventura, 13, IT50145, Florence, Italy
[*]Correspondence: juliana.lobop@gmail.com

Abstract. The study was aimed at design and development of an energy efficient hybrid solar dryer suitable for drying of organic Conilon coffee placed in the town of Seropédica, Rio de Janeiro, Brazil. The energy efficiency and the drying efficiency were the evaluation criteria for thermal performance of the hybrid solar dryer during the coffee drying. Temperature and relative humidity (RH) of the drying and ambient air, solar radiation intensity and coffee weight loss were monitored during the drying process. The process occurred over six consecutive days; the drying time was from 07:00 to 17:00 h, totalling 120 h of operation with an intermittent period (at night) of 14 h. During intermittence, the exhaust system kept off and solar collector and drying chamber sealed. The effective drying period took 60 h, with temperature and RH, respectively, of 38.3 °C and 60.6% outlet of the solar collector, 32.7 °C and 72.2% outlet drying chamber and 27.8 °C and 74.5% ambient air. The maximum temperature in the solar collector and drying chamber reached 54 and 47.7 °C, respectively, with an ambient air temperature of 32 °C at 12:00 h. These values showing temperature increase 22.2 °C in solar collector and 10 ºC drying chamber. The mean variation for the reduction in RH between the drying air inside the solar collector and the ambient air was 28%, while in the chamber obtained in a range of 10.5% at 13:00 h. The solar collector and dryer chamber efficiency were 29.1 and 40.8%, respectively, while the overall dryer efficiency 39.7%.

Key words: organic Conilon coffee, drying, sustainable processing, energy efficiency.

INTRODUCTION

In the processing of coffee fruits there are different methods to obtain sensory characteristics to be consumed as a beverage. Among the methods, those that make up the post-harvest processing can be highlighted. The first stage can be divided into dry pre-processing to obtain natural grain and washing pre-processing generating peeled, pulped and mucilage-free coffee (Lima Filho et al., 2015). These stages is followed by drying of the coffee fruit, in which there is a reduction in their moisture content, thus leading to reductions in chemical reactions and in the proliferation of microorganisms that often deteriorate the final product (Borém et al., 2013, Nakayama et al., 2020). Coffee is one of the products with highest costs in the drying process, not only due to the high initial moisture content but also because the structural characteristics of fruits and grains are susceptible to damage that can depreciate the quality of the dry product, decreasing its commercial value (Palacin et al., 2009).

Specifically, conventional methods of drying coffee can be on the ground (earth and concrete) and in mechanical dryers. The sun drying and air natural stages at the ground is possible in environments with low relative humidity and little cloudiness, having as main advantage the saving of energy. However, this type of drying is a relatively slow process that can lead to considerable losses of product quality, besides requiring extensive areas and long drying time (Deeto et al., 2018). On the other hand, dryers that use energy sources through electricity, firewood or fossil fuels avoid the problems of ground terraces, but they are equipment that increase production costs, harmful to the environment and generate energy dependence for producers (Moreira et al., 2019).

Nowadays, sustainable food processing is becoming an increasingly important issue in developing countries. Within this concept, solar drying is able to meet the growing demand for healthy and low-cost natural foods (Azouma et al., 2019). In view of energy issues, an alternative to the drying process is the use of solar dryers because it is a process that uses renewable and non-polluting energy sources (Altobelli et al., 2014, Azouma et al., 2019). Solar dryers for agricultural products are the most useful device from the point of view of energy conservation that not only saves energy, but also drying time, occupying less area, improving product quality and the employee’s lives (Kant et al., 2016; Camelo et al., 2019; Moreira et al., 2019). In Brazil, solar drying of agricultural products becomes a promising methodology due to the use of the abundance of solar radiation (Alves et al., 2019). With this it is possible to convert solar energy into thermal energy in the solar collector coupled to the dryer and to heat the ambient air (Camelo et al., 2019). Therefore, solar dryers are an alternative to current conventional drying methods for coffee (Moreira et al., 2019).

Solar drying is based on the use of direct and indirect dryers with natural or forced convection, making it possible to control the drying rate (Kumar et al., 2016; Lingayat et al., 2020a). In the first dryer, the solar collector and drying chamber perform the same function with the incidence of radiation directly on the agricultural product (Almeida et al., 2016). These dryers have advantages such as simple construction and low cost, but they present greater product deterioration, slower drying and loss of efficiency due to decreased transmittivity of the glass lid from condensation and moisture (Sandali et al., 2019; Lingayat et al., 2020b). In contrast, in the indirect dryer, the radiation does not act directly on the agricultural product, which results in quality improvements, besides reducing drying time and contaminants, ideal characteristics for coffee drying (Lingayat et al., 2017).

Furthermore, solar dryers can be classified as hybrids in terms of how they are activated by means of energy. In other words, hybrids can be mentioned, in which different forms of generation obtain the same type of energy, whether electrical or thermal (Montero et al., 2010; Oliveira et al., 2019). In addition, hybrid active mode enabled a considerable reduction in drying time, being an aspect to take into account for its use during low solar radiation or at night time (Montero et al., 2015). Hybrid dryers are a viable option as they can make use of solar thermal energy, in heating the drying air, and electrical energy by conventional source or photovoltaic plates, to activate the exhaust system, making that this system is more flexible and economical than the conventional one (Oliveira et al., 2019). Different design and performance evaluation of hybrid dryer has been studies. Solar energy during peak sunshine hours and liquefied petroleum gas (LPG) water heater as auxiliary heat source during low sunshine hours was evaluated to drying of shrimps. In this hybrid dryer, solar system supplied 73.93% of the energy requirement of the solar-LPG hybrid dryer for shrimp drying (Murali et al., 2019).

In association with the construction, design and performance evaluation of different types of dryers, one must take into account the efficiency of these technologies when drying agricultural products. In a study for the development and technical-economic evaluation of an electric hybrid solar dryer for tomato cultivation, Boughali et al. (2009) verified the influence of the increase in air flow on the efficiency of the dryer, thus obtaining efficiency of up to 47.5% for a flow of 2 m s^{-1}. The authors also conclude that under the conditions evaluated, the return on investment was 1.27 years compared to the estimated dryer life of 15 years, indicating that it is a viable option for drying agricultural products.

Currently, several studies are being developed to improve and increase the efficiency of solar dryers through the search for materials that allow greater transfer and conduction of heat. However, complex material combinations make these dryer designs less sustainable and more economical. Khanlari et al. (2020a) mention that when drying agricultural products, temperature is a limiting factor. Thus, evaluating a tube-type air heater associated with the greenhouse dryer, showed a maximum efficiency of 56.77% for an air flow of 0.015 kg s^{-1} and reducing the drying time by 30%.

Evaluating the solar drying of cucumber fruits (*Solanum muricatum* L.), two dryers were developed, an indirect double-pass dryer (DIPSD) and another indirect double-pass dryer with modification of the mesh absorber (DPISDMA). The solar dryer showed an average efficiency of the collector between 70 and 80%, and the addition of the mesh with a thickness of 5 mm improved the thermal performance of the collector, allowing a better quality drying of the cucumber fruits (Güler et al. 2020). By studying the drying behavior of celery (*Apium Graveolens* L.) in a parallel pass solar dryer (PPSC), deflectors were added to the dryer in order to improve thermal performance. The dryer during the evaluation presented instantaneous efficiency of 84.3% for higher flow and higher thermal efficiency as more deflectors are added (Khanlari et al., 2020b).

The drying process and the dynamics of the internal mass transfer mechanisms are specific to each product (Dermirpolate, 2019). There are still few studies on the behavior of coffee drying in such dryers, so in general there is the need for technical and operational information, such as knowledge on the intermittence of the process and on the performance of these dryers (Amunugoda et al., 2013; Shalaby & Bek, 2014; Camelo et al., 2019, Montero et al., 2019). Thus, the objective was to developing a hybrid solar-electric dryer (HSED) for effective use on coffee drying applications. For that purpose, it was studied the thermal efficiency of the solar collector and of the drying chamber, and, subsequently, the overall thermal efficiency of the hybrid solar-electric dryer (HSED) during the drying of conilon coffee.

MATHERIAL AND METHODS

The experiment was conducted at the Laboratory of Rural Electrification and Alternative Energies and at the Laboratory of Storage of Agricultural Products of the Institute of Technology (IT)/Department of Engineering (DE) of the Federal Rural University of Rio de Janeiro (UFRRJ), Campus of Seropédica - Rio de Janeiro, Brazil. The climate of the region is classified as Aw according to Köppen's classification, with average annual temperature of 24.5 °C (Carvalho et al., 2006).

Emcapa 8121 clonal variety of Conilon coffee (*Coffea canephora* Pierre ex Froehner) harvested from organic production systems was used in the experiment. Fruits were harvested manually coming from the Agroecological Farm km 49, located in the municipality of Seropédica, state of Rio de Janeiro. Two types of coffee preparation were analyzed: washed cherry, where the skin and part of the mucilage were removed before they were dried at the HSED and natural coffee, where the fruits were harvested at the green, beginning maturation, and mature stages and taken to the drying at the HSED. The performance of the developed hybrid solar dryer was evaluated using natural (0.88 ± 1 wb, decimal wet base) and washed organic Conilon coffee (0.83 ± 1 wb), until the coffee reached 0.09 ± 1 wb.

The HSED consists of solar collector, drying chamber, exhaust system and photovoltaic panel with solar tracker. In order to make greater use of the incidence of solar radiation for a maximum period of 12 h, the face of the solar collector was installed pointing North with a tilting angle equal to the latitude of the municipality of Seropédica - RJ (23°), plus 15° (Fig. 1).

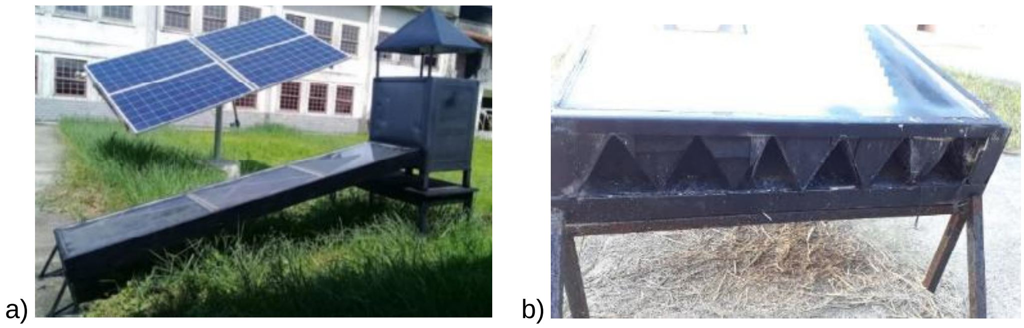

Figure 1. Hybrid solar-electric dryer (HSED) a) Solar collector, drying chamber, photovoltaic panel and b) Conductive air channels of solar collector drying.

The solar collector consists of a rectangular aluminum plate, with dimensions of 0.68×3.00×0.14 m (width × length × height). The adopted solar collector was sized so that an area of 8 m^2 of solar collector is required for each cubic meter of the drying chamber, forming the ratio of 1 m^3:8 m^2, as adopted by Oliveira et al. (2019). The solar radiation-absorbing surface consists of a corrugated aluminum structure in a triangular profile with dimensions of 0.10×0.08 m (base × height) and thickness of the 0.01 m, painted matte black. The surface area exposed to solar radiation consists of a transparent, flat glass plate (0.004 m thick) with area of 2.04 m^2. The absorpsivity and transmissivity of the flat glass plate was 0.07 and 0.85, respectively. The ambient air travels in the thermal fluid circuit in the solar collector through the six lower channels of the absorbing surface to receive thermal energy to the drying chamber. The upper channels of the absorbing surface are sealed so that the ambient air passes only through the lower triangular section. The cross-section area of the solar collector was determined as a function of the quantity and triangular area of the six drying air-conducting channels, being equal to 0.024 m^2.

The drying chamber was made of metal, lined with a glass wool (thermal conductivity - 0.04 W $(m\,K)^{-1}$), and had dimensions of 1.79×1.01×0.85 m (width × height × depth), which resulted in an area of 1.80 m^2 and a volume of 1.54 m^3. Inside it there are three trays containing nine removable metal basket with oblong holes to hold agricultural products, equally distanced from each other. The baskets have a screened bottom to allow the passage of the drying air, through the sample.

There is a rectangular entrance at the bottom of the drying chamber with dimensions of 0.815×0.185 m to fit a connection duct between the solar collector. In the upper part of the chamber, an exhaust fan was installed, with a power of 144 W, in order to guarantee the forced convection of the drying air inside. The exhaust fan accompanies a Dimmer in the form of a potentiometer (Speed Control) that allows to control the rotation of the device.

In order to generate electrical energy to drive the exhaust fan, the photovoltaic system with a 500 W solar tracker was installed. In addition to these electrical energy generating components, the hybrid system consists of a charge controller, batteries and a sinusoidal inverter. The energy storage in batteries guarantees the reliability of the system, as they allow to consume this energy in seasons when no wind is verified. The charge controller manages and controls the charging and discharging process of the battery bank. This controller allows the batteries to be fully charged and prevents them from being discharged below a safe value.

Monitoring of drying air and ambient air parameters

Throughout the drying process, the solar collector and drying chamber of the HSED were monitored for temperature ($T_{air\ dry}$), relative humidity ($RH_{air\ dry}$) and drying air velocity ($V_{air\ dry}$). Ambient air was monitored for temperature ($T_{air\ amb}$), relative humidity ($RH_{air\ amb}$), light intensity and solar radiation. The parameters were obtained at regular periods every hour. Thermocouples connected to a millivoltmeter with accuracy of ± 0.1 °C were used to monitor $T_{air\ dry}$ and $T_{air\ amb}$. $RH_{air\ dry}$ and $RH_{air\ amb}$ were measured using an MTH-1380 thermo-hygrometer. $V_{air\ dry}$ was monitored with a Minipa MDA II digital thermo-anemometer every hour throughout the effective drying period, in order to keep it fixed at 0.98 m s^{-1}. In case of variation, the adjustment of the drying air speed was carried out with the Dimmer attached to the exhaust fan. This value of the present study has been used by Mirzaee et al. (2010), who satisfactorily described the apricot drying curve through a logarithmic model, and by Kant et al. (2016) for the indirect solar drying of potatoes.

Solar radiation data along the solar drying period were obtained from the National Institute of Meteorology (INMET), coming from the automatic weather station of Agricultural Ecology, located in the municipality of Seropédica, Rio de Janeiro, Brazil. This weather station is situated 2.73 km away from the IT of UFRRJ.

Adopted procedure for coffee drying

Initially, the removable basket of each tray were filled with coffee fruits, forming a thin layer of 0.03 m. Then, the trays were arranged in the drying chamber to start the process. The baskets were periodically removed every hour to be weighed during the drying process. The condition of hygroscopic equilibrium was considered so that the variation in the mass of the baskets with coffee did not exceed 0.01 g for three times consecutive weighing procedures, where a final water content of 0.09 ± 1% wb was reached.

The solar drying of the samples was carried out in six consecutive days, being from 07:00 to 17:00 h, totaling 120 h of operation. At night, when the exhaust system was turned off and the solar collector and drying chamber were sealed in order to avoid external interference in the internal microclimate, it was considered an intermittence of 14 h (between 17:00 and 7:00 h). The effective drying time of the coffee, without considering the intermittence period, was 60 h.

Thermal performance of the HSED

After collecting the drying parameters, the thermal efficiency of the solar collector, drying chamber and the overall thermal efficiency of the HSED were evaluated.

Thermal efficiency of the solar collector

The thermal efficiency of the solar collector was determined according to the ratio between the useful energy supplied and the incident solar energy along the drying period (Eq. 1).

$$\eta_c = \frac{E_u}{E_i} = \frac{\int P_{u\,col}\,dt}{A_d \int I_t\,dt} = \frac{P_{u\,col}}{P_i} = \frac{\dot{m} \times c_p \times (T_o - T_i)}{I_t \times A_d} \qquad (1)$$

where η_c – Thermal efficiency of the collector; E_u – Useful energy supplied by the solar collector along the drying period t; E_i – Incident solar energy on the solar collector along the drying period t; $P_{u\,col}$ – Useful energy gain of the collector, W; A_d – Surface area of the solar collector exposed to solar radiation, m²; I_t – Solar radiation on the tilted surface, W m^{-2}; P_i – Potential related to solar energy, W; $\dot{m}$ – Mass flow rate of the air, kg s^{-1}; c_p – Specific heat of the air, J (kg °C)$^{-1}$; T_o – Outlet temperature of the collector, ºC and T_i – Inlet temperature of the collector, °C.

Eq. 2 was adopted to calculate ṁ (Montero et al., 2010).

$$\dot{m} = \rho \times A_c \times v_m \qquad (2)$$

where ρ – Specific mass of the incoming air of the solar collector, kg m^{-3}; A_c – Transverse area of the solar collector, m² and v_m – Average air velocity at the inlet of the solar collector, m s^{-1}.

The ρ was determined as a function of the inlet temperature of the solar collector, according to Eq. 3 (Montero et al., 2010).

$$\rho = \frac{353.44}{T_i + 273.15} \qquad (3)$$

According to the study conducted by Silveira (2016), the efficiency of the solar collector was evaluated considering the insulation of the system does not allow air leakage. The air inside the solar collector behaves as an ideal gas at constant pressure, and the transmittance-absorbance between the glass and the absorbing plate is negligible. The radiation measured on a flat surface (weather station) is the same for the tilted surface. A value of 1,006 J (kg °C)$^{-1}$ was adopted for the specific heat of the air to calculate the efficiency of the collector (Silveira, 2016).

Thermal efficiency of the drying chamber

The thermal efficiency of the HSED drying chamber was determined considering the useful energy gain obtained, potential related to solar energy and to the power required by the exhaust (Eq. 4).

$$\eta_{chm} = \frac{P_{u\,chm}}{P_{u\,col} + P_e} = \frac{\dot{m}_w \times l_v}{P_{u\,col} + P_e} \tag{4}$$

where η_{chm} – Thermal efficiency of the drying chamber; $P_{u\,chm}$ – Useful energy gain of the drying chamber, W; P_e – Exhaust power, W; $\dot{m}_w$ – Water evaporation rate in the grains, kg s^{-1} and l_v – Latent heat of water evaporation at the air saturation temperature, J kg^{-1}.

To calculate the thermal efficiency of the drying chamber, a value of 2,256 J kg^{-1} was adopted for the latent heat of water evaporation at the air saturation temperature. Eq. 5 was used to determine $\dot{m}_w$.

$$\dot{m}_w = \dot{m}_{chm} \times (AM_o - AM_i) \tag{5}$$

where $\dot{m}_{chm}$ – Mass flow rate of the air in the drying chamber, kg s^{-1}; AM_o – Outlet absolute moisture of the drying chamber, decimal and AM_i – Inlet absolute moisture of the drying chamber, decimal.

Equal 6 was used to determine $\dot{m}_{chm}$.

$$\dot{m}_{chm} = \rho_{chm} \times v_{m\,chm} \times A_{chm} \tag{6}$$

where ρ_{chm} – Specific mass of moist air for the drying chamber, kg m^{-3}; $v_{m\,chm}$ – Average air velocity in the drying chamber, m s^{-1} and A_{chm} – Area of the drying chamber, m^2.

The ρ_{chm} was determined as a function of T_{ichm} according to Eq. 7 (Montero et al., 2010).

$$\rho_{chm} = \frac{353.44}{T_{e\,chm} + 273.15} \tag{7}$$

Overall thermal efficiency of the HSED

The overall thermal efficiency of the hybrid solar-electric dryer was determined considering the useful energy gain of the drying chamber, the potential related to solar energy and the power of the exhaust (Eq. 8).

$$\eta_g = \frac{P_{u\,chm}}{P_i + P_e} \tag{8}$$

RESULTS AND DISCUSSION

It was observed that during the solar drying of conilon coffee, the ambient temperature did not vary along the six days of process, averaging 27.8 °C. The average minimum temperature reached was 20.0 °C, at 7:00 h, and the average maximum was 31.6 °C, from 12:00 to 14:00 h. From 14:00 h the ambient temperature decreased until reaching 25.3 °C at 17:00 h (Fig. 2).

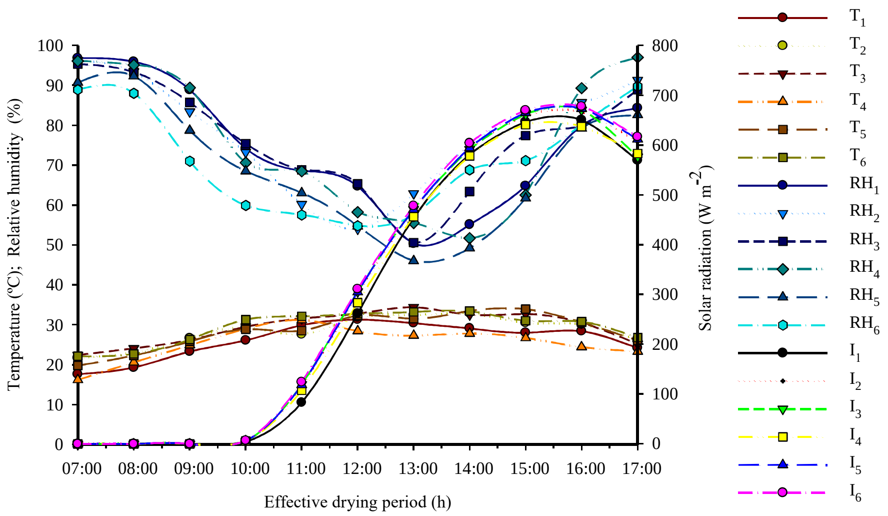

Figure 2. Temperature (°C), relative humidity (%) and global solar radiation (W m^{-2}) over the drying period: T_n – Temperature; RH_n – Relative humidity; I_n – Solar radiation; n – drying day.

Regarding the relative humidity, it can be observed that this drying indicator showed the same behavior over the six days of the process, with an average of 74.5%. The highest values of relative humidity occurred was 94.0% at 07:00 h, and the minimum was 53.8% at 13:00 h.

The average global solar radiation obtained during the drying period of coffee in the HSED was approximately 306.9 W m^{-2}, with peaked was 662.3 W m^{-2} at 16:00 h. The period of maximum average value of global radiation does not coincide with that achieved by the temperature. Furthermore, it can be observed that in the daytime between 07:00 and 10:00 h there was low availability of radiant energy, with an average of 0.5 W m^{-2}. In the period of availability of solar energy (11:00 to 17:00 h), the average global solar radiation was 482.0 W m^{-2} (Fig. 2). Lingayat et al. (2017) when using indirect solar dryer (solar flat plate air collector with V-corrugated absorption plates, insulated drying chamber, and chimney for exhaust air) for banana drying in India obtained maximum and average incident solar radiation values of 1,219.1 and 897.4 W m^{-2}, respectively.

It was verified that environmental conditions are favorable to coffee drying, since the period of higher temperature coincides with lower value of relative humidity and higher availability of solar energy. Additionally, on the fourth day of drying, there was a low incidence of rain, leading to lower temperatures from 12:00 h. In the evaluation of the solar dryer thermal efficiency low incidence of rain, including collector and drying chamber, it is essential to take into account the environmental conditions, such as temperature, relative humidity and radiation, as well as the geographical location (Altobelli et al., 2014).

In specific case of coffee drying, in Brazil, its harvest occurs in the months between May and August (autumn/winter season), so there are excellent environmental conditions such as high level of solar radiation and low level of rainfall. In order to maintain its quality for processing and, subsequently, marketing at any period of the year, coffee is immediately dried. Thus, the drying period of the different lots of conilon coffee are consistent with the Brazilian reality in any season for the metropolitan region of Rio de Janeiro, Brazil.

Thermal efficiency of the solar collector

The thermal efficiency of the solar collector can be influenced by its size, mode of operation, geographical location, mass flow rate, temperature, relative humidity and local radiation (Montero et al., 2010; Lingayat et al., 2017). Fig. 3 shows the curve of drying air temperature (inlet, middle and outlet of the solar collector) along the drying period.

The ambient air temperature and solar collector's inlet temperature did not show great variations among themselves during the coffee drying period, being the average of 27.9 ± 0.02 °C. In contrast, the average temperature in the middle and at the outlet of the solar collector were respectively 10 and 27% higher than that of the inlet.

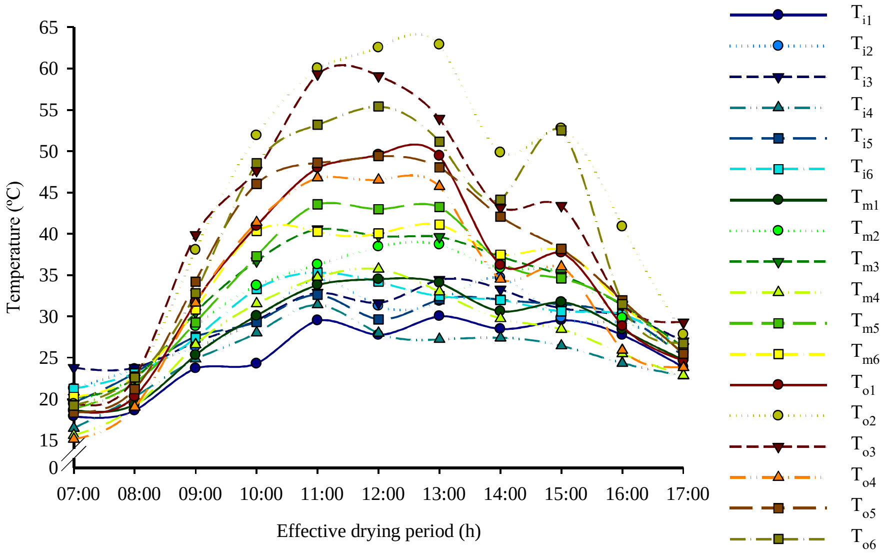

Figure 3. Temperature (°C) as function of effective drying period in the solar collector: T_n – Temperature; i – inlet; m – middle; o – outlet; n – drying day.

The highest average temperatures were recorded at noon, being equal to 32 °C for ambient temperature and at the inlet, to 39 °C in the middle and to 54 °C at the outlet of the solar collector. At this moment, an increase of 21.1 °C was observed in the collector's outlet temperature compared to the inlet temperature. Then, there was a reduction in the temperatures, regardless of the data collection position, equal to 25 °C at 17:00 h (Fig. 3). Shuck et al. (2014) evaluated the efficiency of flat solar collector for tobacco drying and considered the inlet temperature of the solar collector as the ambient temperature itself, because there was no significant difference between the two.

In addition to the increase in drying air temperature and global solar radiation, the reduction of relative humidity is a factor that proves the efficiency of the solar collector. Combined with this, indicators such as temperature and relative humidity are tools to be considered when there are variables other than solar radiation taken as energy sources (Altobelli et al., 2014).

Therefore, in Fig. 4 presents the relative humidity recorded at the outlet of the solar collector, which decreased by 33% at 12:00 h, compared to air at the inlet (Fig. 2). In general, the relative humidity of the ambient air and at the inlet of the solar collector showed a difference of no more than 5% at 09:00 and 11:00 h.

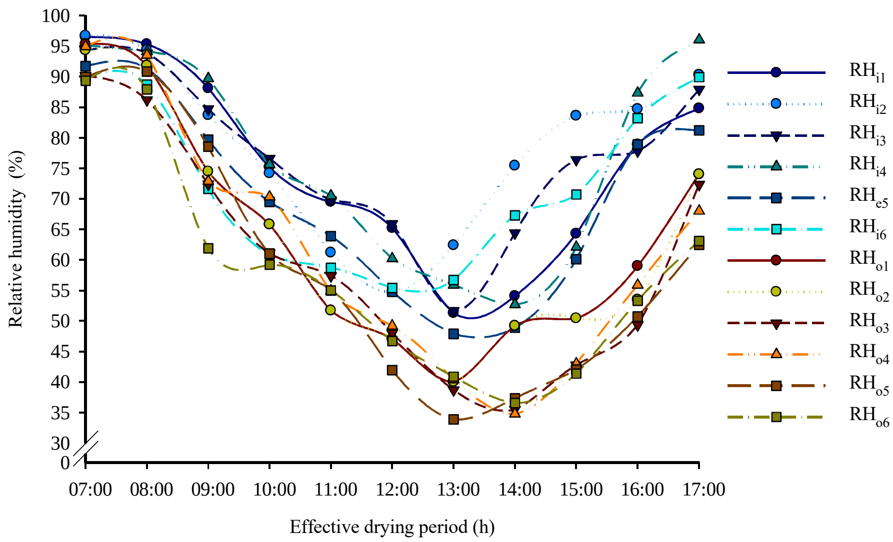

Figure 4. Relative humidity (%) as function of effective drying period in the solar collector: RH_n – Relative humidity; i – inlet; m – middle; o – outlet; n – drying day.

In terms of instantaneous thermal efficiency of the solar collector, at the beginning of the daytime there were average values higher than 100%, equal to 1,201% at 07:00 h, 490% at 08:00 h, -6,187% at 09:00 h and 2,421% at 10:00 h. The high values of instantaneous thermal efficiency of the solar collector in the coffee drying period from 07:00 to 10:00 h can be justified by the combination between low global solar radiation and temperature, as observed in Fig. 2. When determining the thermal efficiency of the solar collector of continuous solar dryer integrated with desiccant thermal storage for drying cocoa beans, Dina et al. (2015) did not adopt the day time due to the low availability of solar energy.

In particular at 11:00 h, there was an increase in global solar radiation, which, together with the variation of temperature (Fig. 2), reduced the efficiency of the solar collector (Fig. 5). However, when considering the six days of coffee drying, the average instantaneous thermal efficiency of the solar collector was 120%, that is, higher than 100%. Thus, for 11:00 h the average instantaneous thermal efficiency was calculated only with daily values below 100%.

Altobelli et al. (2014) evaluated the instantaneous thermal efficiency of the flat solar collector coupled to a dryer in Argentina, considering only values below 100%, since they obtained higher values in the afternoon, as the intensity of solar radiation decreases. These authors also observed a similar behavior with the performance of the system, solar collector and drying chamber, because at the beginning they observed values similar to the total performance, but reached values beyond possible when radiation was zero. Due to the dependence only on solar radiation, the authors considered that the thermal efficiency of the solar collector alone does not adequately describe the behavior of the solar dryer, so the system needs to be considered as a whole to determine the thermal efficiency.

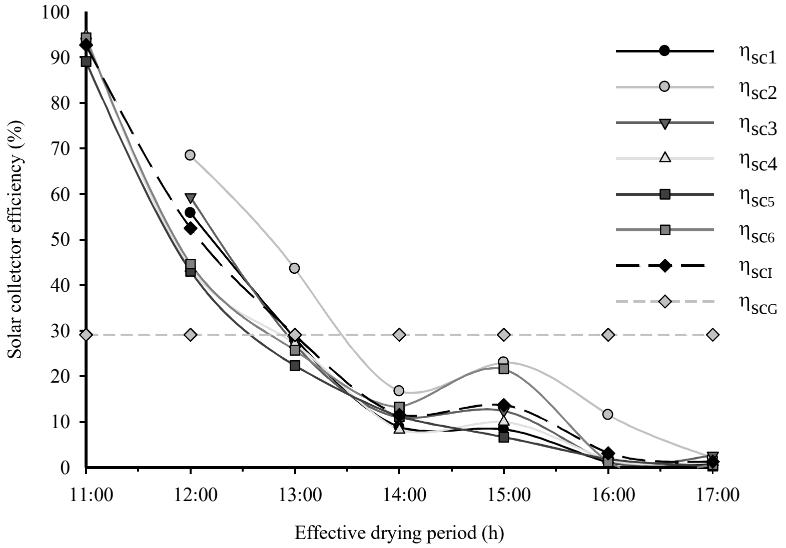

Figure 5. Thermal, instantaneous and global average efficiency of the solar collector throughout the drying period: η_{scn} – Solar collector efficiency; n – drying day; I – Instantaneous; G – Global.

In the drying period from 11:00 to 17:00 h, there was a reduction in the instantaneous thermal efficiency, regardless of the drying day. In calculating the average thermal efficiency of the solar collector at 11:00 am, only the fourth (95%), fifth (89%) and sixth (94%) day of coffee drying was taken into account (Fig. 5). From 12:00 h, the second day showed higher values of instantaneous thermal efficiency. The increase in instantaneous thermal efficiency at 15:00 h, followed by reduction, confirms the interference of the drying indicators, that is, temperature variation associated with higher values of global solar radiation (Fig. 2).

Similar behavior was reported by Kareem et al. (2017), according to whom the instantaneous thermal efficiency of the multi-pass solar air heating collector system for drying of screw-pine leaf (*Pandanus tectorius*) reduced as a function of the drying period, showing 50% efficiency at 09:00 h with solar irradiation close to zero Watts per square meter and temperature (ambient and outlet of the collector) of 20 °C. Demirpolat (2019) analyzed the behavior of apple drying in a convective indirect solar dryer and found that the maximum thermal efficiency of the collector occurred between 12:00 and 13:30 h, with 65% thermal efficiency in the collector.

Oliveira et al. (2019), performing the drying of mangoes in a convective indirect solar dryer, reported that the peak of maximum instantaneous thermal efficiency of solar collector was approximately 60% at 14:00 h at four days of drying, with global solar radiation and ambient temperature ranging from 400 to 600 W m^{-2} and from 35 to 60 °C, respectively. Gulcimen et al. (2016), during the drying of sweet basil in a convective indirect solar dryer, obtained maximum instantaneous efficiency of solar collector of

42% at 13:00 h, with global solar radiation between 720 and 750 W m^{-2} and mass flow rate of 0.012 kg s^{-1}.

The average thermal efficiency of the solar collector of 29% is higher than that found in the literature by Oliveira et al. (2019), who obtained 26% during solar drying, under conditions of average solar radiation of 361 W m^{-2}. This value is also higher than those found by Fudholi et al. (2015), equal to 28%, in the back-passV-groove solar collector coupled in solar drying of red pepper, and by Altobelli et al. (2014), equal to 27%, evaluating drying indicators in northwestern Argentina. On the other hand, Lingayat et al. (2017) evaluated the performance of indirect solar dryer for banana drying obtained average overall efficiency of 31%. The authors conducted the experiment under conditions of average incident radiation of 724 W m^{-2}, more than twice the one mentioned in the present study (306.9 W m^{-2}).

Thermal efficiency values higher than that found in the present study were reported by Hedge et al. (2015), 36% higher. However, these authors adopted thermal systems to maintain the temperature high inside the flat plate solar collector during the period of low solar energy availability and ambient temperature.

Thermal efficiency of the drying chamber

During the solar drying of coffee, it was observed that both the temperature and relative humidity of the drying air show differences when compared at the inlet and outlet of the drying chamber (Fig. 6). The average differences in temperature and relative humidity between drying air at the inlet and at the outlet were 5.7 °C and 1.7%, respectively.

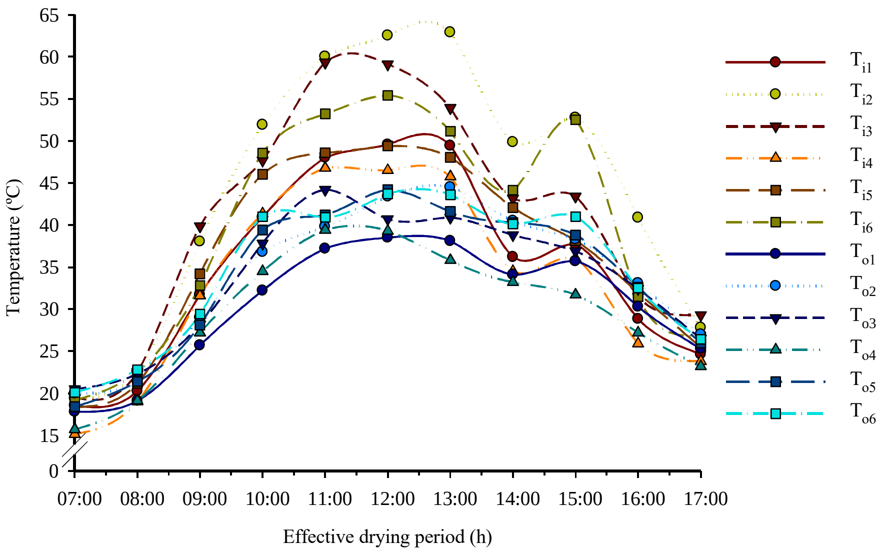

Figure 6. Temperature of the drying air in the SHSE chamber over the drying period: T_n – Temperature; i – inlet; o – outlet; n – drying day.

Furthermore, it can be observed that the highest temperatures and lowest values of relative humidity occurred inside the drying chamber when compared to the air ambient. The highest temperatures at the inlet and outlet of the drying chamber occurred from

11:00 to 13:00 h, while the lowest ones occurred during the early morning and late afternoon (Fig. 6). On the other hand, the minimum relative humidity at the inlet and outlet of the drying chamber occurred at 13:00 h and the maximum values occurred at 07:00 and 17:00 h (Fig. 7).

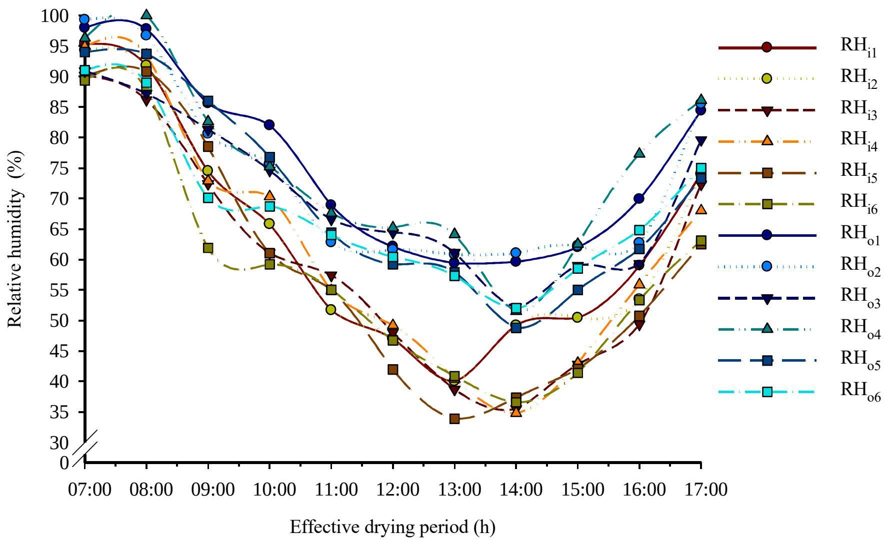

Figure 7. Relative humidity of the drying air in the SHSE chamber over the drying period: RH_n – Relative humidity; i – inlet; o – outlet; n – drying day.

The average value of drying air temperature and UR inside the SHSE chamber was 35.5 °C and 66.4%, respectively. The average maximum temperature reached inside the drying chamber was 47.7 °C at 12:00 h. At that same time, the ambient air had a temperature of 31.6 °C, that is, an increase of 16.1 °C. Regarding the average minimum relative humidity reached in the drying chamber was 39.7% at 13:00 h, with 53.2% in the ambient air, a reduction of 13.5%. The average variation in the temperature increment and the reduction of relative humidity between the drying air inside the chamber and the ambient air was 7.7 °C and 5.5%, respectively. The higher temperature and lower relative humidity inside the drying chamber when compared to the ambient meteorological conditions indicate the capacity of the drying chamber to not lose heat to the environment.

It was found that the relative humidity decreases with the increase of temperature, as evidenced by the air exiting the solar collector and entering the drying chamber. High relative humidity was observed at the outlet of the drying chamber, compared to the inlet, and this can be attributed to the variation in the drying rate of the material as the moisture content decreases.

Dina et al. (2015) evaluated the continuous solar drying of cocoa seeds using a flat-plate solar collector and obtained lower results of thermal variation than those of the present experiment. The authors obtained an increase of 12 °C in the air temperature inside the drying chamber comparison to the ambient. In addition, the increase obtained was also higher than that reported by Shalaby & Bek (2014), who evaluated the performance of an indirect solar dryer and found an increase of 7.5 °C between drying air temperature and ambient temperature.

For the study of the thermal efficiency of the drying chamber for conilon coffee, the average values of temperature, relative humidity, drying air velocity were 38.9 °C, 53.6% and 0.98 m s^{-1}, respectively. As adopted for the solar collector, only the fourth, fifth and sixth day were considered for calculating the average values of the thermal efficiency of the drying chamber at 11:00 h. As expected, the highest average values of instantaneous thermal efficiency occurred at 11:00 and 12:00 h (66.3%), while the lowest at 17 h (17.6%). Considering the six days of coffee drying, the average instantaneous thermal efficiency of the drying chamber was 40.8%.

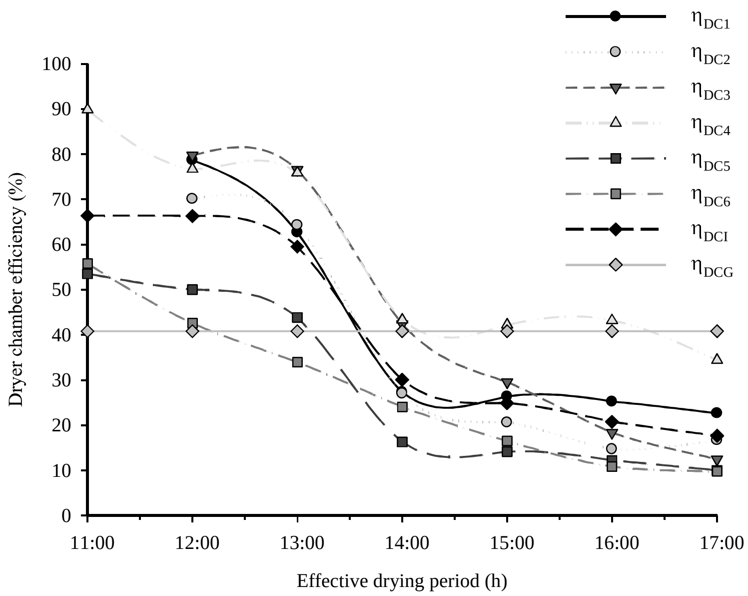

Figure 8. Thermal efficiency of the drying chamber of the hybrid solar-electric dryer over the drying period: η_{DCn} – Dryer chamber efficiency; n – drying day; I – Instantaneous; G – Global.

The maximum and minimum value of instantaneous thermal efficiency reached was 89.8% at 11:00 h on the fourth day and 9.7% at 17:00 h on the six day, respectively (Fig. 8). The high values of instantaneous thermal efficiency in the drying chamber along the coffee drying period from 11:00 to 13:00 h can be justified by the combination between high temperature (Fig. 6) and the reduction in relative humidity (Fig. 7).

In the drying period from 13:00 to 17:00 h, there was a reduction in the instantaneous thermal efficiency, regardless of the drying day. The relative humidity of the air entering the drying chamber was more stable until 10:00 h, while that of the air inside the drying chamber continuously decreases until about 13:00 h (Fig. 7). Such behavior may be an indication that most of the moisture in the product had already evaporated at that time, although solar radiation has increased at the same time, leading to a reduction in the thermal efficiency of the drying chamber (Fig. 8). Musembi et al. (2016), when analyzing an indirect solar dryer by natural convection for medium latitudes, obtained similar results. The authors observed stability in the inlet relative humidity during the first 40 min of the drying days, noting that the value in the air of the drying chamber decreases until 15:00 h. The average overall thermal efficiency of the drying chamber was 48.8% for the six days of drying, value that is within the range obtained by Hao et al. (2020), evaluating a hybrid dryer for lemon drying.

Overall thermal efficiency of the HSED

Regarding the overall thermal efficiency, the same profile shown by the drying chamber can be observed (Fig. 8). The highest values of global thermal efficiency occurred at 11:00 am from the fourth day of solar drying. For this period of solar drying, the average global efficiency was 64.1%. Considering the six days of coffee drying, the average overall thermal efficiency of the drying chamber was 39.7% (Fig. 9).

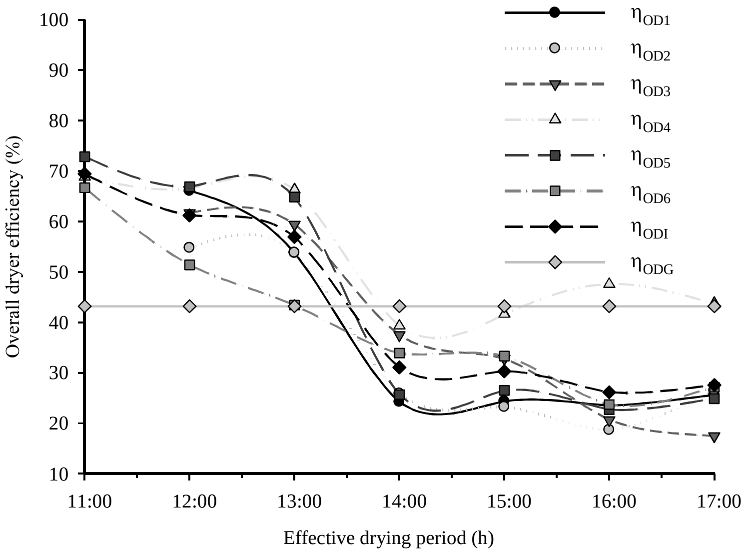

Figure 9. Overall thermal efficiency of the hybrid solar-electric dryer over the drying period: η_{ODn} – Overall dryer efficiency; n – drying day; I – Instantaneous; G – Global.

Lingayat et al. (2017) and Altobelli et al. (2014) obtained values of 22.38 and 17%, respectively, for the average overall thermal efficiency of their experiments. This confirms that the local climatic conditions of Brazil are excellent for the use of indirect solar drying, combining the drying indicators such as temperature, relative humidity and solar radiation.

Mass reduction in natural and pulped coffees

Fig. 10 shows the reduction in the mass of natural and pulped grains, respectively, over the drying period. It should be noted that the initial mass of the natural grain (Fig. 10, a) is lower than the pulped grain (Fig. 10, b), being 291.2 and 295.4 g, respectively, at 7:00 am on the first day. However, it did not affect the solar drying process. This difference in initial mass is justified due to the wet treatment used for pulping.

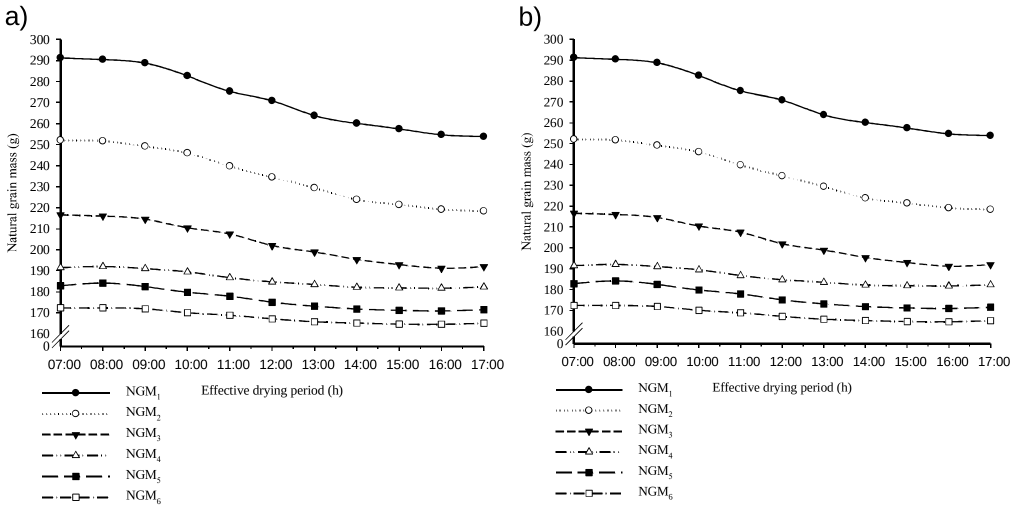

Figure 10. Reduction in the mass of a) natural and b) washed grains throughout the drying period: NGM_n – Natural grain mass; WGM_n – Washed grain mass; n – drying day.

It is also observed that, during the drying of the conilon coffee, the period of intermittence did not interfere with the mass loss of the product. However, greater mass loss can be observed on the first two days in both pulped and natural grains. The highest rate of water removal in the first two days is due to the initial elimination of free water from the grain surface.

It can be observed that there was a reduction in grain mass every day of solar drying, being more pronounced on the first day. Thus, it can be inferred that the rainy season did not interfere in the coffee drying as commonly occurs in conventional processes. On earth and suspended terraces in the rainy season, coffee drying is delayed, which leads to an increase in the period and a probable interference in the final quality of the product.

It can also be verified that, from the third day, the mass of both lots of grains remained constant along the drying period. Regarding the effect of the intermittence period, the product did not absorb moisture, as reported by Camelo et al. (2019) in solar drying of banana. The final masses of natural grains and pulped grains were 165.1 and 186.8 g, respectively. Thus, it can be considered that on the last day the product reached the hygroscopic equilibrium with the environment, and the results are similar to those obtained by Silvia et al. (2019) for the drying of conilon coffee fruits in a hybrid dryer.

CONCLUSIONS

The studied electric solar hybrid dryer proved efficient in the drying process of conillon coffee. Results show that the temperature increases 18.1 °C in the solar collector and in the drying chamber of 21.3 °C, allowing the coffee to dry at acceptable and ideal temperatures for the drying process. The average variation for the reduction of RH between the drying air inside the solar collector and the ambient air was 10.8%, while in the chamber obtained in the range of 13.5% at 13:00 h. During the drying of conilon coffee, the intermittence period did not interfere in the loss of mass of the product. Regarding the values obtained for efficiency, the solar collector and dryer chamber efficiency were 27.1 and 45.3%, respectively, while the overall dryer efficiency 39.7%. The drying of coffee is one of the processes with the greatest attention due to the direct influence on the quality of the drink and marketing price. As most of the producers still use conventional drying methods, the data obtained in the present study allow us to say the hybrid solar-electric dryer proved to be an economically viable and economical tool for processing a differentiated and gourmet coffee in small rural. It is seen that HSED is promising in view of sustainability and this simple structure can be utilized as an alternative to drying applications.

ACKNOWLEDGEMENTS. The authors wish to thank the Conselho Nacional de Desenvolvimento Científico e Tecnológico (CNPq) that provided support for this research project.

REFERENCES

Almeida, I.B., Lima, M.A.A. & Souza, L.G.M. 2016. Solar dryer development built from recycled material. *Holos* **4**, 197–205 (in Portuguese).

Altobelli, F., Condorí, M., Duran, G. & Martinez, C. 2014. Solar dryer efficiency considering the total drying potential. Application of this potential as a resource indicator in north-western Argentina. *Solar Energy* **105**, 742–759.

Alves, R.A., Queiroz, A.J.M., Figueiredo, R.M.F., Silva, W.P. & Gomes, J. P. 2019. Solar drying of cowpea bean combined with drying in a heat accumulator dryer. *Revista Brasileira de Engenharia Agrícola e Ambiental* **9**, 709–715.

Amunugoda, P.N.R.J., Senanayake, N.S., Wilson Wijeratnam, R.S. & Kulatunga, K.D.G. 2013. Quality enhancement of dehydrated products through the modification of solar tunnel dryer for continuous operation in rural communities. *International Journal of Energy Engineering* **1**, 7–14.

Azouma, Y.O., Drigalski, L., Jegla, Z., Reppich, M., Turek, V. & Weiz, 2019. M. Indirect convective solar drying process of pineapples as part of circular economy strategy. *Energies* **12**, 2841.

Borém, F.M., Oliveira, P.D., Isquierdo, E.P., Giomo, G.S., Saath, R. & Cardoso, R.A. 2013. Scanning electron microscopy of coffee beans subjected to different forms of processing and drying. *Coffee Science* **2**, 227–237 (in Portuguese).

Boughali, S., Benmoussa, H., Bouchekima, B., Mennouche, D., Bouguettaia, H. & Bechki, D. 2009. Crop drying by indirect active hybrid solar - electrical dryer in the eastern Algerian Septentrional Sahara. *Solar Energy* **83**, 2223–2232.

Camelo, R.S.S., Paes, J.L., Brás, M.R.S., Bruggianesi, G. & Guimarães, C.L. 2019. Kinetics drying of silver banana (*Musa* spp.) in hybrid dryer. *Ciência Agronômica* **3**, 353–360.

Carvalho, D.F., Silva, L.D.B., Folegatti, M.V., Costa, J.R. & Cruz, F.A. 2009. Evaluation of reference evapotranspiration in the Seropédica-RJ region, using weighing lysimeter. *Revista Brasileira de Agrometeorologia* **14**, 108–116 (in Portuguese).

Deeto, S., Thepa, S., Monyakul, V. & Songprakorp, R. 2018. The experimental new hybrid solar dryer and hot water storage system of thin layer coffee bean dehumidification. *Renewable Energy* **115**, 954–968.

Demirpolat, A.B. 2019. Investigation of mass transfer with different models in a solar energy food-drying system. *Energies* **12**, 3447–3461.

Dina, S.F., Ambarita, H., Napitupulu, F.H. & Kawai, H. 2015. Study on effective ness of continuous solar dryer integrated with desiccant thermal storage for drying cocoa beans. *Case Studies in Thermal Engineering* **5**, 32–40.

Fudholi, A., Sopian, K., Bakhtyar, B., Gabbasa, M., Othman, M.Y. & Ruslan, M.H. Review of solar drying systems with air based solar collectors in Malasia. 2015. *Renewable and Sustainable Energy Reviews* **51**, 1191–1204.

Gulcimen, F., Karakaya, H. & Durmus, A. 2016. Drying of sweet basil with solar air collectors. *Renewable Energy* **93**, 77–86.

Güler, H.O., Sözen, A., Tuncer, A.D., Afshari, F. & Khanlari, A. 2020. Experimental and CFD survey of indirect solar dryer modified with low-cost iron mesh. *Solar Energy* **197**, 371–384.

Hao, W., Liu, S., Mi, B. & Lai, Y. 2020. Mathematical modeling and performance analysis of a new hybrid solar dryer of lemon slices for controlling drying temperature. *Energies* **13**, 350–373.

Hedge, V.N., Hosur, V.S., Rathod, S.K., Harsoor, P.A. & Narayana, K.B. 2015. Design, fabrication and performance evaluation of solar dryer for banana. *Energy* **1**, 5–23.

Kant, K., Shukla, A., Sharma, A., Kumarm A. & Jain, A. 2016. Thermal energy storage based solar drying systems: A review. *Innovative Food Science and Emerging Technologies* **34**, 86–99.

Kareem, M.W., Habib, K., Sopian, K. & Ruslan, M.H. 2017. Multi-pass solar air heating collector system for drying of screw-pine leaf (*Pandanus tectorius*). *Renewable Energy* **112**, 413–424.

Khanlari, A, Sözen, A, Şirin, C, Tuncer, A.D. & Gungor, A. 2020a. Performance enhancement of a greenhouse dryer: Analysis of a cost-effective alternative solar air heater. *Journal of Cleaner Production* **19**, 1–30.

Khanlari, A., Güler H.O., Tuncer, A.D., Sirin, C., Bilge Y.C., Yılmaz, Y. & Güngor A. 2020b. Experimental and numerical study of the effect of integrating plus-shaped perforated baffles to solar air collector in drying application. *Renewable Energy* **145**, 1677–1692.

Kumar, M., Sansaniwal, S.K. & Khatak, P. 2016. Progress in solar dryers for drying various commodities. *Renewable and Sustainable Energy Reviews* **55**, 346–60.

Lima Filho, T., Lucia, S.M.D., Saraiva, S.H. & Lima, R.M. 2015. Physico-chemical characterization of espresso coffee beverage prepared from blends of arabica and conilon coffees. *Revista Ceres* **4**, 333–339 (in Portuguese).

Lingayat, A., Chandramohan, V.P. & Raju, V.R.K. 2017. Design, Development and performance of indirect type solar dryer for banana drying. *Energy Procedia* **109**, 409–416.

Lingayat, A., Chandramohan, V.P., Raju, V.R.K. & Kumar, A. 2020a. Development of indirect type solar dryer and experiments for estimation of drying parameters of apple and watermelon. *Thermal Science and Engineering Progress* **16**, 1–65.

Lingayat, A., Chandramohan, V.P., Raju, V.R.K. & Meda, V. 2020b. A review on indirect type solar dryers for agricultural crops – Dryer setup, its performance, energy storage and important highlights. *Applied Energy* **258**, 1–22.

Mirzaee, E., Rafiee, S. & Keyhani, A. 2010. Evaluation and selection of thin-layer models for drying kinetics of apricot (cv. NASIRY). *Agric Eng Int: CIGR Journal* **12**, 111–116.

Montero, I, Miranda, M.T., Sepúlveda, F.J., Arranz, J.I., Rojas, C.V. & Nogales, S. 2015. Solar dryer application for olive oil mill wastes. Energies **8**, 14049–14063.

Montero, I., Blanco, J., Miranda, T, Rojasa, S. & Celma, A.R. 2010. Design, construction and performance testing of a solar dryer for agroindustrial by-products. *Energy Conversion and Management* **7**, 1510–1521.

Moreira, D.H.F., Freitas, F.F., Landy, C.C.R. & Charbel, A.L.T. 2019. Analysis of coffee drying in direct passive solar dryer. *Brazilian Journal of Development* **9**, 16556–16573.

Murali, S., Amulya, P.R., Alfiya, P.V., Delfiya, D.S.A. & Samuel, P.M. 2019. Design and Performance Evaluation of Solar - LPG Hybrid Dryer for Drying of Shrimps, *Renewable Energy* **147**, 2417–2428.

Musembi, M.N., Kiptoo, K.S. & Yuichi, N. 2016. Design and analysis of solar dryer for mid-latitude region. *Energy Procedia* **100**, p. 98–110.
Nakayama, C.C., Teixeira, A.A., Teixeira, R.R., Reis, M. Montero, A. & Bueno, J. 2020. Microorganism succession at different coffee drying stages and its influence on the beverage. *Brazilian Journal of Development* **6**, 2402–2418.
Oliveira, L.C.T.G., Paes, J.L., Guimarães, C.L., Camelo, R.S.S., Misquita, Í.S. & Lovisi, T.A.P. 2019. Evaluation of the efficiency of the flat solar collector coupled in hybrid dryer. *Energia Solar e Eólica*, vol. 01. Ponta Grossa (PR): Atena Editora, Cap.**13**, 194–211 (in Portuguese).
Palacin, J.J.F., Lacerda Filho, A.F., Melo, E.C. & Teixeira, E. C. 2009. Secagem combinada de café cereja descascado. *Engenharia na Agricultura* **3**, 244–258 (in Portuguese).
Sandali, M., Boubekri, A., Mennouche, D. & Gherraf, N. 2019. Improvement of a direct solar dryer performance using a geothermal water heat exchanger as supplementary energetic supply. An experimental investigation and simulation study. *Renewable Energy* **10**, 186–196.
Schuck, M.L.R., Santos, J.P., Soares, R.M.D., Zófoli, G.R., Garlet, L. & Gricoletti, G.C. 2014. Solar collector for air pre-heating on drying systems case study - curing tobacco. *Extensão Rural* **21**, 106–130 (in Portuguese).
Shalaby, S.M. & Bek, M.A. 2014. Experimental investigation of a novel indirect solar dryer implementing PCM as energy storage medium. *Energy Conversionand Management* **83**, 1–8.
Silveira, L.R. 2016. *Modeling of a solar dryer for agricultural products with thermal energy storage system.* PhD Thesis Thesis in Engenharia de Sistemas Agrícolas, Piracicaba: Escola Superior de Agricultura Luiz de Queiroz, University of São Paulo, 60 pp. (in Portuguese).
Silvia, E., Yuwana, Y. & Bosman, S. 2019. Performance of modified hybrid solar dryer on the drying process of robusta cherry coffee. *Journal Agroindustrial* **9**, 94–101 (in Indonesian).